ANALYSIS OF TILTROTOR AIRFRAME VIBRATORY LOADS TRANSMITTED BY THE WING-PROPROTOR SYSTEM

M. Gennaretti, M. Molica Colella, & G. Bernardini
University Roma Tre, DIMI, Rome, Italy

ABSTRACT

This paper presents a procedure for the analysis of vibratory loads generated by a wing-proprotor system. It is applicable for the investigation of tiltrotors both in airplane and helicopter modes. The aeroelastic formulation applied takes into account the mechanical mutual influence between elastic wing and rotor blades, along with the aerodynamic interactional effects that are dominated by the impact between wing and proprotor wake vortices. Beam-like models are used to describe wing and rotor blades structural dynamics, while a boundary integral formulation suited for configurations where strong body-vortex interactions occur is applied to determine the aerodynamic loads. A harmonic balance approach is applied to determine the corresponding aeroelastic response. The aerodynamic solver is first validated by correlation with experimental and numerical results available in the literature, and then coupled with the aeroelastic solver to examine the vibrating loads arising on the wing-proprotor system, focusing the attention on the importance of the different terms contributing to them.

1. INTRODUCTION

The last 30 years have experienced continuous attempts to obtain reliable VTOL vehicles both for civil and military use. Among the different solutions the tiltrotors have revealed to be a suitable answer to get a perfect combination between helicopters manoeuvrability and airplane high flight-speed. As the required capabilities increase, so do the requests for stability and comfort and the need for prediction tools able to predict the structural and aerodynamic behaviour.

The objective of the paper is to present a numerical procedure for the aeroelastic analysis of tiltrotor configurations. It is aimed at the prediction of the vibratory loads transmitted to the fuselage at the wing root, which are due to the hub loads generated by the proprotor, along with the aerodynamic interactions between the wing and the wake of the rotor blades. These are obtained by combining an aeroelastic solver for wing-proprotor configurations with an aerodynamic prediction tool that is able to analyse flows in which strong body/wake interaction occurs. The aeroelastic tool determines the trim wing and rotor blades elastic deflections that, in turn, yield inertial loads and are used to impose the impenetrability boundary conditions in the aerodynamic solver. Elastic-beam and aerodynamic quasi-steady models described by Hodges and Dowell (1974) and Hodges and Ormiston (1976) are applied to derive the set of coupled, nonlinear, integro–differential aeroelastic equations governing bending and torsion of wing and rotor blades. The interactional aerodynamic tool is based on the boundary integral formulation for the velocity potential presented by Gennaretti and Bernardini (2007), and applied in the past to the aerodynamic/aeroacustic analysis of helicopter configurations where strong blade/wake interaction occurs (Bernardini et al, 2007). This formulation is fully 3D, can be applied to configurations in arbitrary motion, and allows the calculation of both wake distortion and pressure field.

The aeroelastic code has been validated in the past by Molica (2006) through comparison with the numerical analysis presented by Johnson (1974), while the aerodynamic formulation has been validated by comparison with experimental data concerning helicopter rotors in descent flight (Gennaretti and Bernardini, 2007). Here, the objective of the numerical investigation is twofold: first, the boundary integral formulation for potential flows is validated by comparison with experimental and numerical data available in the literature concerning a wing-proprotor system in airplane configuration, then the aeroelastic formulation is applied to determine the vibrating loads arising in airplane and helicopter mode, with the aim to investigate the importance of the different terms contributing to them. These results are an improvement of the preliminary ones recently presented by Bernardini et al (2007).

2. VIBRATORY LOADS ANALYSIS

The evaluation of the vibratory loads is obtained by combining an aeroelastic solver with an aerodynamic tool that is able to capture the effects of the aerodynamic interference between rotor and wing, including the strong rotor-wake/wing interaction. The aeroelastic tool uses a quasi-steady aerodynamic model coupled with the equations governing the structural dynamics of the wing/pylon/rotor system; it yields both the inertial component of the vibratory loads and the elastic deformations to be used in the impenetrability surface conditions in the aerodynamic solver which, in turn, evaluates the aerodynamic component of the vibratory loads. Then, if these aerodynamic loads are used as input in the aeroelastic code, such procedure may be applied iteratively until convergence is reached. The aeroelastic and the aerodynamic solvers are briefly described in the following.

2.1. The Aeroelastic Formulation

Beam-like models are applied to describe the structural dynamics of both wing and rotor blades. They are based on the nonlinear bending-torsion equations of motion presented by Hodges and Dowell (1974), that are valid for straight, slender, homogeneous, isotropic, nonuniform, twisted wing/blades. Retaining second order terms after the application of an ordering scheme that drops third-order terms not contributing to damping, and assuming radial displacements as simply geometric consequences of the transverse bending deflections (Hodges and Ormiston, 1976), the final form of the dynamic system is a set of coupled nonlinear integro-partial differential equations having as unknowns in-plane and out-of-plane displacements of the elastic axis, along with the cross-section elastic torsion. It is suitable for describing the response of beam-like structures undergoing significant deflections.

Both wing and rotor aerodynamic loads are simulated through 2D, quasi-steady, aerodynamic models (with wake-inflow corrections in the rotor blade analysis, to take into account the 3D trailing vortices influence). The kinematics of the rotor blades is strongly affected by the motion of the wing section to which the rotor is attached to through the pylon structure. Thus, both aerodynamic and inertial blade forcing terms are significantly dependent on the elastic deformation of the wing. On the other hand, in addition to the aerodynamic loads, wing dynamics is forced by forces and moments transmitted by the rotor at the wing section where the pylon is located and by the inertial effects due to the pylon mass.

The combination of wing and rotor blade aeroelastic models yields a set of equations governing the aeroelasticity of the wing/pylon/rotor system which are strongly coupled. Their solution is obtained through the application of the Galërkin method for the space discretization, followed by a harmonic balance approach for the time integration (Gennaretti and Bernardini, 2006).

2.2. The Aerodynamic Formulation

The aerodynamic field of wing-rotor systems is dominated by the interactional effects occurring between rotor blades and wing. Periodic blade passages close to the wing are a first source of oscillations in the pressure field over wing and proprotor blades (even in case of airplane mode configurations), but the main source of wing unsteady aerodynamic loads is given by the impact between wing and rotor wake vortices. Indeed, the wing located behind the propeller is massively impinged by the wake vorticity released by the rotor blades: this generates local flow and pressure perturbations that, in turn, yield a significant contribution to the vibrating loads. The analysis of aerodynamic problems involving the strong interaction between vortices and bodies is a complex task that requires the application of suited solver.

In this work the unsteady wing-rotor aerodynamics has been analysed through a boundary integral formulation for potential flows introduced by Gennaretti and Bernardini (2007) as a development of the formulation presented by Morino (1974), in order to overcome instabilities of the numerical solution arising in case of impingement between wake and body surfaces. It introduces the decomposition of the potential field into an incident field, φ_I, and a scattered field, φ_S. The scattered potential is generated by sources and doublets over the body surfaces and by doublets over portions of the body wakes that are very close to the trailing edges from which they emanated (near wake, $\mathcal{S}_W^N$). The incident potential is generated by doublets over the complementary wake regions that compose the far wakes, $\mathcal{S}_W^F$. These are the wake portions that may come in contact with other body surfaces (note that, in the present analysis, body surface denotes rotor blades and wing surfaces, while the wake surface includes wakes from both rotor blades and wing). The scattered potential is discontin-

uous across $\mathcal{S}_W^N$, whereas the incident potential is discontinuous across $\mathcal{S}_W^F$. Hence, as demonstrated by Gennaretti and Bernardini (2007), for $\varphi = \varphi_I + \varphi_S$ the scattered potential is obtained by

$$\begin{aligned}\varphi_S(\mathbf{x},t) &= \int_{\mathcal{S}_B}\left[G\,(\chi-\chi_I)-\varphi_S\frac{\partial G}{\partial n}\right]\mathrm{d}\mathcal{S}(\mathbf{y}) \\ &- \int_{\mathcal{S}_W^N}\Delta\varphi_S\,\frac{\partial G}{\partial n}\,\mathrm{d}\mathcal{S}(\mathbf{y})\end{aligned}$$

where $\chi = \mathbf{v}\cdot\mathbf{n}$ accounts for the impenetrability boundary condition (with $\mathbf{v}$ denoting the body velocity due to rigid and elastic body motion), while $\chi_I = \mathbf{u}_I\cdot\mathbf{n}$, with the velocity induced by the far wake, $\mathbf{u}_I = \nabla\varphi_I$, given by

$$\mathbf{u}_I(\mathbf{x},t) = -\nabla\int_{\mathcal{S}_W^F}\Delta\varphi_S(\mathbf{y}_W^{TE},t-\theta)\,\frac{\partial G}{\partial n}\,\mathrm{d}\mathcal{S}(\mathbf{y}) \quad (1)$$

The incident potential influences the scattered one by the induced-velocity term, χ_I, and, in turn, the scattered potential influences the incident one by its trailing-edge discontinuity that is convected along the wake and yields the intensity of the doublet distribution over the far wake.

Obtaining the zero-th order discrete form of equation (1) by using N panels over the far wakes and recalling the vortex-doublet equivalence, the incident velocity field may be evaluated through the following expression

$$\mathbf{u}_I(\mathbf{x},t)\approx -\sum_{n=1}^{N}\Delta\varphi_S(\mathbf{y}_{W_n}^{TE},t-\theta_n)\int_{\mathcal{C}_n}\nabla_{\mathbf{x}}G\times\mathrm{d}\mathbf{y}$$

where $\mathcal{C}_n$ denotes the contour line of the n-th far wake panel, $\mathbf{y}_{W_n}^{TE}$ is the trailing edge position where the wake material point currently in $\mathbf{y}_{W_n}$ emanated at time $t-\theta_n$, and $\nabla_{\mathbf{x}}$ denotes the operation of gradient with respect to the variable $\mathbf{x}$. This equation represents the velocity field given by the Biot-Savart law applied to the vortices having the shape of the far wake panel contours and intensity $\Delta\varphi_S(\mathbf{y}_{W_n}^{TE},t-\theta_n)$. The final step of the formulation presented by Gennaretti and Bernardini (2007) consists of introducing in these vortices a finite-thickness core where a regular distribution of the induced velocity is assured, along with a stable and regular solution even in body-vortex impact conditions (Gennaretti and Bernardini, 2007) (it is worth reminding that only the far wake may experience such events). The description of the wake influence through the use of finite-core vortices is a way to include also diffusivity and vortex-stretching effects that, otherwise, would not be taken into account in a potential-flows aerodynamic formulation.

Equation 1 is solved numerically by boundary elements, *i.e.,* by dividing $\mathcal{S}_B$ and $\mathcal{S}_W^N$ into quadrilateral panels, assuming φ_S, χ, χ_I and $\Delta\varphi_S$ to be piecewise constant (zero-th order, boundary element method - BEM), and imposing the equation to be satisfied at the center of each body element (collocation method). Once the potential field is known, the Bernoulli theorem yields the pressure distribution and the integration over the body surface gives the corresponding aerodynamic loads.

3. NUMERICAL INVESTIGATION

The numerical investigation concerns both the validation of the unsteady BEM formulation for predictions of wing-rotor aerodynamics and the analysis of the vibrating loads arising at airplane-mode and helicopter-mode flight configurations.

3.1. Validation of BEM aerodynamic solver

The wing-propeller configuration examined is that investigated experimentally by Chiaramonte et al (1996), which consists of a propeller/nacelle/half-wing test model. The propeller has four blades with radius $R = 0.425$m, NACA 64A408 airfoil sections and the twist distribution given by Fratello et al (1991). The half wing has RA18-43N1L1 airfoil sections, length $L_w = 1.0$m and constant chord $c = 1.02$m (Chiaramonte et al, 1996). The results presented in the following concern the airplane-mode configuration, with freestream velocity $V = 17.2$m/s and propeller rotating clockwise (seen from downstream) with angular speed $\Omega = 1362$RPM (see Chiaramonte et al (1996) for further details). Figure 1 shows the comparison between the measured and the predicted mean pressure coefficient, $\bar{c}_p$, along the upper and lower sides of the section located at a distance of 0.5m from the wing root, which is very close to the region of tip-vortex passage (*i.e.,* approximately behind the rotor disk edge). In addition to the results obtained through the present approach, figure 1 depicts also the numerical predictions presented by Benneceur (1995). On the upper side of the section the results from the present formulation are in good agreement with the experimental ones, and seem to correlate slightly better than those by Benneceur (1995). On the lower side the

pressure peak close to the leading edge is a bit overestimated by the present approach, similarly to the predictions by Benneceur (1995); however, after the first 10% portion of the chord our numerical prediction is in excellent agreement with the experimental data.

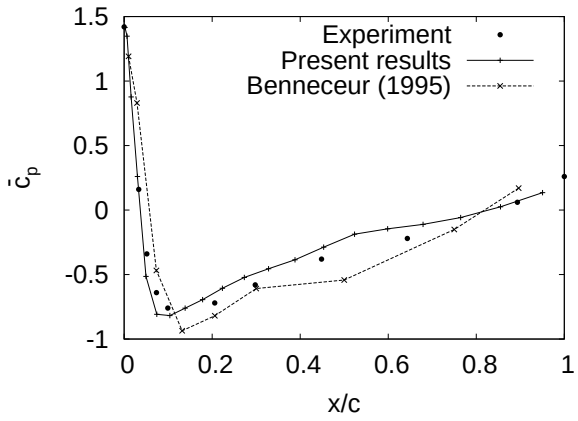

Upper side

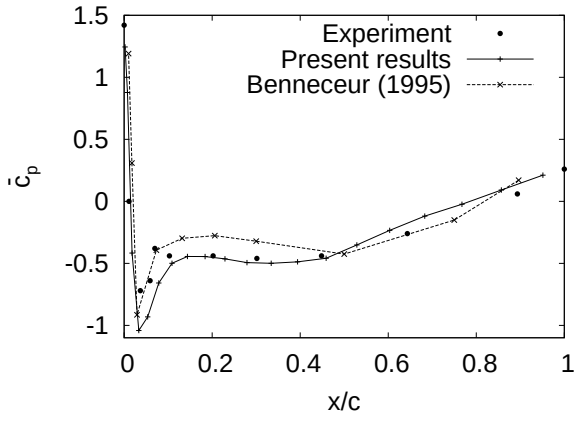

Lower side

Figure 1: *Mean pressure coefficient at* $y = 0.5m$.

Concerning the prediction of the pressure time histories over the wing surface, figure 2 presents the comparison between our numerical results and the experimental data given by Chiaramonte et al (1996), for three transducers located on the upper side of the wing at the section closest to the tip-vortex passage region (indicated by Chiaramonte et al (1996) as transducers number 1, 5 and 10). Although a higher frequency content is observed in the predictions related to the transducer 5 and a phase shift of about 35 deg is present (probably due to the difference between the numerical and experimental initial acquisition times), the agreement between the numerical results and the experimental data is quite good showing, in particular, a satisfactory prediction of the attenuation of amplitude of pressure oscillations from leading edge to trailing edge (these pressure oscillations come from the interaction between the rotor wake and the wing).

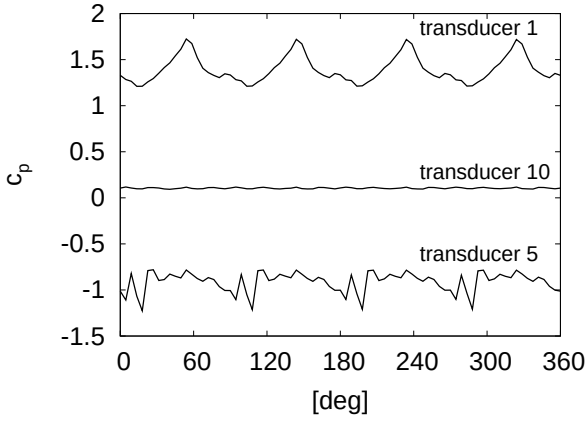

Numerical

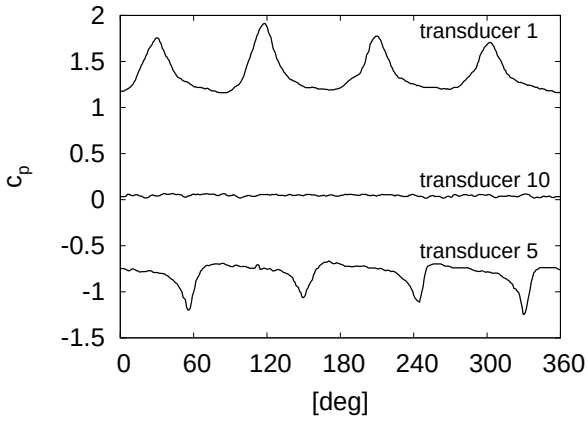

Experimental

Figure 2: *Pressure coefficient time histories at* $y = 0.5m$.

3.2. Analysis of vibrating loads

The analysis of the vibrating loads transmitted by the wing-proprotor system to the airframe has been performed by considering the gimballed-rotor model examined by Johnson (1974). For this configuration, the aeroelastic model applied here has already been validated in terms of stability characteristics (Molica, 2006), showing (using the same aerodynamic model) an excellent agreement with the results presented by Johnson (1974) and Johnson (1975). The wing considered has length $L_w = 5.092$m and chord $c = 1.58$m,

while the three-bladed gimballed rotor has radius $R = 3.82$m (see Johnson (1974) for further details on the geometrical and structural properties).

First, the wing-proprotor in airplane mode has been examined. In this flight condition the freestream velocity is $V = 128.5$m/s and the propeller rotates with $\Omega = 458$RPM. The wing angle

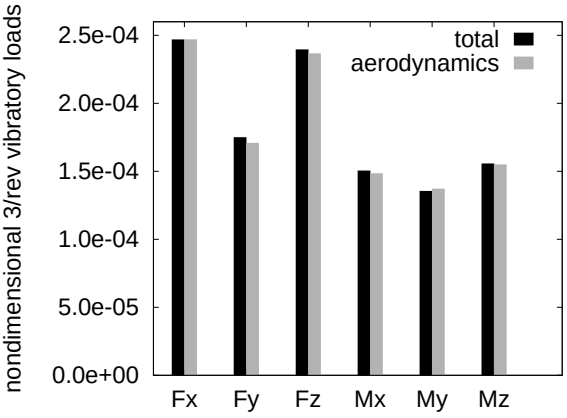

Figure 3: *Loads in airplane mode.*

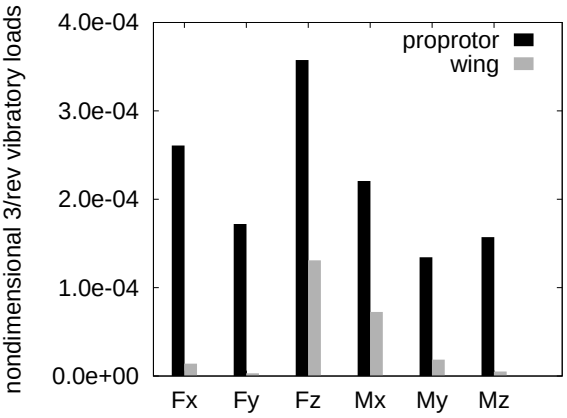

Figure 4: *Aerodynamic loads in airplane mode.*

of attack is equal to 3° and the proprotor axis is aligned with the freestream. Figure 3 shows the predicted $3/rev$ harmonics of the loads transmitted to the airframe at the shear center of the wing root section due to the inertial and aerodynamic effects (total) and to the only aerodynamic effects. Note that the x-axis of the reference frame is aligned with the freestream, the z-axis is in the vertical plane directed upwards and the y-axis is along the wing span. As expected, in this configuration the inertial contribution to the vibrating loads is very marginal, these being dominated by aerodynamics. Figure 4 depicts the contribution to the aerodynamics loads given by the wing and the proprotor separately. It demonstrates that the most important vibrating loads come from the propeller and are due to the interaction with the wing, that makes the rotor flow asymmetric. Further, the impact between rotor wake and wing produces not negligible vibrating loads over the wing surface, particularly in terms of vertical force and chordwise bending moment.

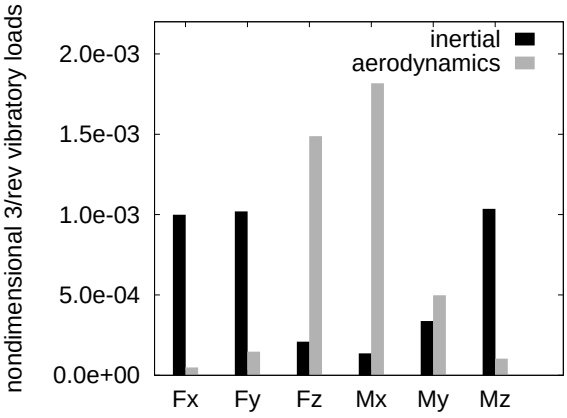

Figure 5: *Loads in helicopter mode.*

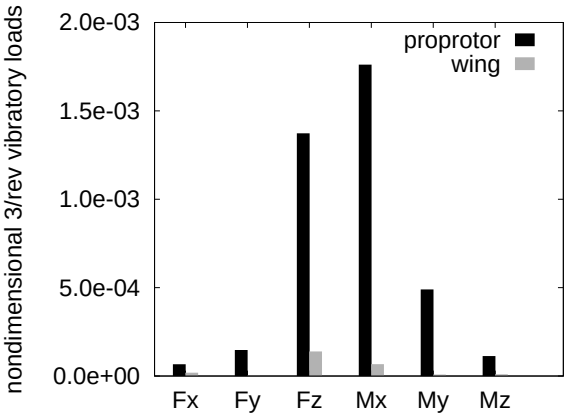

Figure 6: *Aerodynamic loads in helicopter mode.*

In addition, the numerical investigation has proven that, in this flight condition, the harmonic aerodynamic loads are barely affected by the elastic deformations of wing and proprotor blades.

Then, the wing-proprotor has been examined in helicopter mode, with freestream velocity $V = 30.84$m/s, propeller angular velocity $\Omega = 600$RPM and shaft angle $\alpha_{sh} = -9°$. Figure 5 shows that, differently from the cruise configuration, the vibratory inertial loads are not negligible with respect to the aerodynamic ones; moreover, figure 6 shows that the contribution from the proprotor is the most part of the vibratory loads, being the contribution from the wing very small as, in this case, there is not a strong

interaction with the proprotor wake (the wake does not impinge the wing).

Finally note that, as expected, the results shown above demonstrate that the highest vibratory load levels appear in helicopter-mode flight, where the most asymmetric flow condition arises.

4. CONCLUSIONS

A formulation for the aerodynamic/aeroelastic analysis of wing-rotor systems has been presented. The aerodynamic solver has been validated by correlation with experimental data available in the literature. The aeroelastic response has been evaluated in order to examine the vibratory loads transmitted to a tiltrotor airframe by the wing-proprotor system. The aerodynamic BEM formulation has been proven to be able to predict with very good accuracy the mean pressure distribution over the wing surface impinged by the proprotor wake, with the exception of some localized minor discrepancies at the lower side leading edge regions behind the rotor disk. The pressure time histories over the wing has been predicted with a good accuracy as well, showing a satisfactory prediction of the attenuation of the pressure fluctuation amplitudes from leading to trailing edge. A higher frequency content has been observed in some regions of the wing, and this point deserves further research effort, mostly aimed to investigate about the necessity of a more sophisticated algorithm to model the viscous effects in the interaction between the wing boundary layer and the rotor wake. The vibrating loads analysis has shown that in cruise flight the inertial and elastic deformation effects are negligible, while significant aerodynamic contributions come from the propeller and the wing because of interactional effects, including the rotor wake impingement on the wing surface. Important contributions from the inertial effects have been obtained in helicopter mode configuration. Akin to the airplane-mode case, in helicopter mode the highest contribution to the loads transmitted to the airframe comes from the proprotor.

5. REFERENCES

Hodges, D.H., Dowell, E.H., 1974, Nonlinear Equation for the Elastic Bending and Torsion of Twisted nonuniform Rotor Blades. *NASA TN D-7818.*

Hodges, D.H., Ormiston, R.A., 1976, Stability of Elastic Bending and Torsion of Uniform Cantilever Rotor Blades in Hover with Variable Structural Coupling. *NASA TN D-8192.*

Gennaretti, M., Bernardini, G., 2007, Novel Boundary Integral Formulation for Blade-Vortex Interaction Aerodynamics of Helicopter Rotors. *AIAA Journal* **45**: 1169-1176.

Bernardini, G., Serafini, J., Iannniello, S., Gennaretti, M., 2007, Assessment of Computational Models for the Effect of Aeroelasticity on BVI Noise Prediction. *Int'l J. of Aeroacoustics* **6**: 199-222.

Molica Colella, M., 2006, Sviluppo di una Metodologia per l'Analisi Aeroelastica di Configurazioni Ala-Rotore. *Master Thesis*, University Roma Tre. (in Italian)

Johnson, W., 1974, Dynamics of Tilting Proprotor Aircraft in Cruise Flight. *NASA TN D-7677.*

Bernardini, G, Molica Colella, M., Gennaretti, M., 2007, Wing-Proprotor Aeroelastic Modeling for Vibratory Loads Analysis. *XIX Congresso Nazionale AIDAA*, Forlí, Italy.

Gennaretti, M., Bernardini, G., 2006, Aeroelastic Response of Helicopter Rotors Using a 3-D Unsteady Aerodynamic Solver. *The Aeronautical Journal* **110**: 793-801.

Morino, L., 1974, A General Theory of Unsteady Compressible Potential Aerodynamics. *NASA CR-2464.*

Chiaramonte, J.Y., Favier, D., Maresca, C., Benneceur, S., 1996, Aerodynamic Interaction Study of the Propeller/Wing Under Different Flow Configuration. *Journal of Aircraft* **33**: 46-53.

Fratello, G., Favier, D., Maresca, C., 1991, Experimental and Numerical Study of the Propeller/Fixed Wing Interaction. *Journal of Aircraft 28*: 365-373.

Benneceur, S., 1995, Contribution à l'Étude des Interactions Aérodynamiques sur un Avion-Convertible (Configuration Hélice/Nacelle/Demi-Aile. *Thèse de Docteur de l'Université*, Université d'Aix-Marseille II. (in French)

Johnson, W., 1975, Analytical Modeling Requirements for Tilting Proprotor Aircraft Dynamics. *NASA TN D-8013.*